Biofilm 6 (2023) 100165

Contents lists available at ScienceDirect

Biofilm

journal homepage: www.sciencedirect.com/journal/biofilm

Selected flavonoids exhibit antibiofilm and antibacterial effects against *Vibrio* by disrupting membrane integrity, virulence and metabolic activities

Olajide Sunday Faleye, Jin-Hyung Lee, Jintae Lee *

School of Chemical Engineering, Yeungnam University, 280 Daehak-Ro, Gyeongsan, 38541, Republic of Korea

ARTICLE INFO

Keywords:
Antibiofilm
Antimicrobial
Antivirulence
Flavonoid derivatives
Foodborne pathogens
Vibrio parahaemolyticus

ABSTRACT

Vibrio parahaemolyticus is a high-risk foodborne pathogen associated with raw or undercooked seafoods and its biofilm forming potential has become a threat to food safety and economic values. Hence, this study aims to examine the antibacterial and antibiofilm activities as well as virulence inhibitory effects of selected flavonoids against *V. parahaemolyticus*. Out of the sixteen flavonoid derivatives, 6-aminoflavone (6-AF), 3,2-dihydroxyflavone (3,2-DHF) and 2,2-dihydroxy-4-methoxybenzophenone (DHMB) were found as active biofilm inhibitors. 3,2-DHF and DHMB had minimum inhibitory concentrations of 20 and 50 μg/mL respectively against *Vibrio* planktonic cells and displayed superior antibacterial activities to standard controls. Also, they disrupted preformed biofilms and suppressed virulence properties including motilities, cell hydrophobicity and aggregation. They impaired iron acquisition mechanism and hemolysin production at sub-MICs as supported by transcriptomic studies. Interestingly, the flavonoids interfered with the metabolic activity, cell division and membrane permeability to exert antibiofilm and antibacterial activities. 6-AF and 3,2-DHF were non-toxic in the *C. elegans* model and showed excellent capacity to protect shrimps from biodeterioration. Furthermore, the flavonoids inhibited biofilm formation by *V. harveyi*, *Staphylococcus aureus* and *Salmonella typhimurium* and the mixed-species biofilm with *Vibrio*. This study discovered flavonoid derivatives, especially 3,2-DHF as potential bioactive compounds capable of offering protection from risks associated with biofilm formation by *V. parahaemolyticus* and other food pathogens.

1. Introduction

Microbial seafood contamination is unarguably one of the foremost causes of food-related outbreaks which has negatively impacted the safety, supply chain and sustainability of seafood production. In particular, *Vibrio parahaemolyticus* has caused devastating outbreaks of global prominence and continues to threaten the seafood industry. *V. parahaemolyticus* is a Gram-negative, halophilic, facultative γ-proteobacterium that inhabits marine and estuarine environments with the capacity to cause acute gastroenteritis upon consumption of contaminated raw or undercooked seafoods [1]. The bacterium is prevalent in the United States, China, and Korea and it is the leading cause of *Vibrio* poisoning or infection associated with seafood ingestion [2,3]. More recently, it was isolated in Africa from fresh and ready-to-eat foods, and its latest threat concerns the emergence of a new epidemic strain O4: KUT-recAin, which was isolated from diarrhea patients in China [4,5]. Its capacity to form strong biofilms was correlated to antibiotic resistance and high horizontal gene transfer [6,7].

Biofilm formation is composed of surface aggregation of cells embedded in extracellular polymeric materials where they are shielded from various stressors, such as osmolarity, pH changes, disinfectants, and antibiotics, and enhance the horizontal exchange of resistant genes [8]. Biofilm of *V. parahaemolyticus* has become an established source of seafood contamination [9]. It was reported to colonize food contacted surfaces and seafoods, including shrimps, shellfish, gizzard shad, oysters, mussels, pomfret and crabs, due to their high nutritional contents [6,10]. The biofilm state enhances their persistence on food surfaces, diminishes the efficacy of food processing technologies, compromises food safety and increases economic loss [11]. The bacterium is also capable of releasing thermostable direct hemolysins (TDH) which are major biomarkers of pathogenicity [12]. Additionally, its attachment and survival are further aided by a plethora of virulence factors, including adhesion and quorum sensing (QS) factors, extracellular enzymes, effector secretion, and siderophore production which enable survival in iron-deficient environments [13]. Given these attributes and the risk of contamination during harvesting and processing, *Vibrio*

* Corresponding author.
E-mail address: jtlee@ynu.ac.kr (J. Lee).

https://doi.org/10.1016/j.biofilm.2023.100165
Received 28 August 2023; Received in revised form 31 October 2023; Accepted 1 November 2023
Available online 7 November 2023

biofilms pose an ongoing threat to sustainability of seafoods and public health. Thus, effective multifaceted strategies that target biofilm formation and virulence activities are required to ensure the quality and safety of seafood.

Flavonoids, which are secondary metabolites with polyphenolic structures found in fruits, vegetables, and certain beverages, possess a range of pharmacological properties utilized to control human pathogens [14,15]. For instance, fisetin and phloretin suppressed biofilm formation by *Acinetobacter baumannii* [16], morin inhibited biofilm formation by *Vibrio cholera* [17], and neoflavonoids isolated from *Dalbergia melanoxylon* controlled an array of bacterial and fungal pathogens [18]. Flavonoids also inhibited quorum sensing in *Vibrio harveyi* [19]. Due to their antioxidant activities, they are considered as supplements and in food application to limit lipid peroxidation [20]. Thus, demonstrating the relevance of flavonoid derivatives in this study.

3,2-dihydroxyflavone is a natural flavonoid isolated from *Marsdenia tinctoria* and others including onions, tea and citrus fruits [21]. Its antifungal and antiviral activities were reported against *Saccharomyces cerevisiae* and influenza virus respectively [22,23]. It also induced extracellular vesicles which showed wound healing effects from mesenchymal stem cells [24]. Its capacity to increase intracellular glutathione, pluripotent stem cells, improve hematopoietic progenitor cells activity and the natural killer cell induction revealed the safety, antioxidative, and neuroprotective potentials of the flavonoid [25,26]. Despite the forgoing, no information exists on its antibiofilm, and antibacterial activities and no studies have reported its ability to inhibit bacterial virulence and the capacity to ensure safety in food models.

Therefore, in this study, 3,2-dihydroxyflavone and other active flavonoids were identified as potential biofilm, and planktonic cells inhibitors among 16 flavonoid derivatives against *V. parahaemolyticus*. They were further investigated for their capacities to attenuate an array of virulence factors and the potential applications in food model were assessed in shrimp and squid. We examined the toxicity *in-silico* and *in-vivo* using a nematode model and the transcriptomic analysis to decipher their effects on the expressions of biofilm- and virulence-related genes. The possible mechanism of antibacterial action was also investigated. Since biofilm formation in the food industry invariably involves multispecies interactions, the abilities of the flavonoids to control other food-related pathogens, namely, *V. harveyi*, *S. aureus,* and *Salmonella typhi* and the mixed biofilm formation by *V. parahaemolyticus* and *S. aureus* were also exploited.

2. Materials and methods

2.1. Chemicals

The flavonoid derivatives used in the study (Table S1) were obtained from Sigma-Aldrich (St. Louis, United States) or Combi-Blocks (San Diego, United States). Stock solutions (50 mg/mL) were prepared in dimethyl sulfoxide (DMSO) and kept in a refrigerator (−20 °C) until required. Sodium hypochlorite (NaOCl), tetracycline, hexadecyltrimethylammonium bromide (HDTMA), and iron (III) chloride ($FeCl_36H_2O$) were purchased from Sigma-Aldrich (St. Louis, United States) and sodium tripolyphosphate, chrome azurol sulfonate (CAS), and sodium chloride were obtained from Yakuri Pure Chemical (Tokyo), Tokyo Chemical (Japan), and OCI (Seoul), respectively.

2.2. Bacteria and culture conditions

V. parahaemolyticus ATCC 17802, *V. harveyi* ATCC 14412, *S. aureus* ATCC 6538, and *Salmonella typhi* ATCC 13311 were obtained from the American Type Culture Collection (Manassas, USA) and maintained in Luria-Bertani medium (LB medium) (Difco, New Jersey, USA) containing glycerol and stored at −80 °C. For resuscitation and experimental purposes, *Vibrio* spp. was streaked on agar plates, and a single colony was cultured in mLB (LB supplemented with 3 % NaCl) at 30 °C. *S. aureus* and *S. typhi* were treated in the same manner but cultured in LB at 37 °C. All experiments were conducted in triplicate using at least two independent cultures. Solvent DMSO at 0.1 % (v/v) did not inhibit biofilm formation or bacterial growth and thus served as the control.

2.3. Antibiofilm studies

2.3.1. Antibiofilm screening and minimum inhibitory concentration determination

Overnight cultures of *V. parahaemolyticus* were diluted at 1:100 in mLB (10^6 CFU/mL), dispensed (300 μL) into 96-well plates (SPL Life Sciences, Pocheon, Korea), and incubated under a static condition at 30 °C for 24 h in the presence or absence of flavonoid derivatives. After incubation, absorbances were measured at 620 nm for planktonic cell growth. MIC was defined as the lowest concentration at which no visible growth was observed. Biofilm formation was quantified by gently washing plates three times with distilled water (dH_2O) and softly drained. Crystal violet (CV; 0.1 %, 300 μL) was then added to each well and left at room temperature for 20 min. Unbound CV was rinsed with dH_2O, and 95 % ethanol was added to solubilize the attached CV. Absorbances were measured at 570 nm using a Multiskan EX microplate reader (Thermo Fisher Scientific, Waltham, MA, United States) [27]. Using the same procedure, the antibiofilm effects of the selected flavonoids were compared to those of the positive controls namely sodium tripolyphosphate (STPP), tetracycline (TET), and sodium hypochlorite (NaOCl, 10 % available chlorine).

2.3.2. Eradication of age-dependent preformed biofilms

Biofilms were developed in 96-well plates as described in section 2.3.1 in the absence of flavonoid derivatives and incubated for 24 or 48 h at 30 °C. Post incubation, non-attached cells were removed, and biofilms were washed gently with phosphate-buffered saline (PBS, pH 7.4) using a multichannel pipette. Different concentrations of flavonoids in fresh mLB were then dispensed into the wells and incubated for 24 h at 30 °C. Biofilms were then CV stained, and absorbances were recorded at OD_{570}. Similarly, biofilms preformed with shaking on the surfaces of polystyrene tubes for 24 h at 30 °C were gently washed to remove non-adherent cells and carefully rinsed with PBS twice. Attached cells were treated with different concentrations of flavonoids in fresh mLB and incubated at 250 rpm for 24 h at 30 °C. Adherent bacteria on tube surfaces were stained with 0.1 % CV after incubation, rinsed after 20 min and photographed.

2.3.3. Microscopic evaluation of antibiofilm activities

V. parahaemolyticus biofilms were developed in 96-well plates and incubated statically with or without the flavonoid derivatives for 24 h at 30 °C. Planktonic cells were removed, plates carefully rinsed with dH_2O, and the biofilms were examined using the iRiS Digital Cell Imaging System (Logos BioSystems, Anyang, Korea). The images obtained were remodeled as 3-D color-coded images using ImageJ software (available at (https://imagej.nih.gov/ij/index.html)).

To study the morphologies of biofilm cells, biofilms were produced as described above but on the surfaces of nylon membranes (0.3 × 0.3 cm, Merck Millipore, Burlington, USA) which were carefully inserted into 96-well plates containing *V. parahaemolyticus* and incubated with or without flavonoids at 30 °C for 24 h. Cells that adhered to membrane surfaces were prepared as described previously [18], platinum sputtered, and visualized using a scanning electron microscope (Hitachi S-4800, Tokyo, Japan) at 15 kV. The same procedure was repeated to study the mixed biofilm formation involving *V. parahaemolyticus* and *S. aureus*.

2.3.4. Biofilm cell viability assays

Biofilm metabolic viability was evaluated using the triphenyl tetrazolium chloride (TTC) assay [28]. Briefly, *V. parahaemolyticus* biofilms grown in mLB (1:100) were developed in 96-well plates, as described

above, at 30 °C. Non-adherent cells were removed using a multichannel pipette and rinsed twice with mLB. Then, biofilms were exposed to the selected flavonoids diluted in mLB (250 μL) at different concentrations (0, 2, 5, 10 or 20 μg/ml). TTC dye was added to each well to a final concentration of 0.05 % w/v and incubated overnight statically for 24 h at 30 °C. Thereafter, medium was removed, the bound red formazan produced by TTC reduction was dissolved in methanol, and absorbance measured at 500 nm using a Multiskan EX microplate reader. Biofilm cell viabilities were expressed as percentage absorbances versus untreated controls.

2.4. Cell growth and time kill kinetic assays

To assess the flavonoid effects on cell growth, *V. parahaemolyticus* cells were diluted in mLB (1:100), dispensed into 96-well plates (300 μL), and incubated for 24 h at 30 °C with or without the selected flavonoids (0, 2, 5, 10 or 20 μg/ml). Optical densities (ODs) were measured two-hourly at 620 nm for 24 h using a Multiskan EX microplate reader [18].

Time killing assay was performed using log-phase cultures obtained by growing *V. parahaemolyticus* in mLB at 250 rpm for 3 h at 30 °C to an OD of ~0.8. Cells were harvested, washed twice with PBS, diluted in mLB (OD 0.4), exposed to the selected flavonoids (2 × MIC) or 800 μg/mL of NaOCl (the positive control), and incubated at 30 °C. A similar procedure was used to assay cells in the stationary phase, which were grown for 14 h. After exposure for 1, 3, 6, 12, or 24 h, samples were taken, appropriately diluted, spread on mLB agar, and incubated for 24 h at 30 °C. Colonies were then counted and expressed as $\log_{10}$ CFU/mL [29]. In addition, the above procedures were repeated for both growth phases in PBS instead of mLB to determine the effect of the derivatives on non-actively growing cells.

2.5. Activities of the flavonoid derivatives on virulence factors

2.5.1. Bacterial motility assay

The effects of the selected flavonoids on polar flagella-mediated swimming motility were determined by inoculating 1 μL of an overnight culture of *V. parahaemolyticus* centrally on semi-solid mLB plates (0.3% agar) seeded with or without the flavonoids (2 or 10 μg/mL). Swarming assays were performed using the same procedure but on solid mLB plates (0.6% agarose). After incubation for 24 h at 30 °C, the diameters of areas covered by motile cells were measured, recorded, and photographed [30].

2.5.2. Hydrocarbon adhesion assay

Cell surface hydrophobicity (CSH) was determined by assessing the ability of *V. parahaemolyticus* to adhere to hydrocarbons [31]. The bacterium was grown in mLB (2 mL) with or without derivatives and incubated for 24 h at 30 °C. Cells were pelleted at 12,000 rpm for 10 min, washed twice with PBS, and suspended in 4 mL of PBS. Initial OD values (A) were determined at 600 nm using a UV/VIS spectrophotometer (Optizen 2120UV, Korea) before vortexing, and then 1 mL of toluene was added, vigorously mixed, and suspensions were left undisturbed for 30 min to separate into phases. Then, 1 mL of aqueous phases was added to cuvettes, and the ODs (B) were measured at 600 nm. Percentage CSH was calculated using $(A - B)/A \times 100$.

2.5.3. Autoaggregation

Cell autoaggregation was assessed as previously described with some modification [32]. *V. parahaemolyticus* cells were treated and processed as described below in section 2.6.2. Subsequently, cell pellets were washed twice with PBS, adjusted in PBS (4 mL) to an $OD_{initial}$ of ~0.5 (OD_{620}), and incubated for 4 h at 30 °C. Supernatants were gently aliquoted, and absorbances were measured at OD_{620} using a Multiskan EX microplate reader. Percent auto-aggregation was calculated using: % auto-aggregation $= (1 - OD_{treated}/OD_{initial}) \times 100$.

2.5.4. Indole production

V. parahaemolyticus cells were grown with or without the selected flavonoids at 250 rpm and 30 °C for 24 h. Aliquots (1 mL) of cultures were centrifuged at 12,000 rpm for 10 min, and then 300 μL of Kovacs reagent, prepared as described by [33] was added to supernatants and allowed to react for 2 min at room temperature. Then, 50 μL of the pink product was diluted in 1000 μL HCl-amyl alcohol solution obtained from the addition of 35 % HCl (75 mL) to amyl alcohol (225 mL) and absorbances were measured at 540 nm. Indole productions were determined using a standard indole concentration versus absorption curve.

2.5.5. Protease secretion

Briefly, *V. parahaemolyticus* diluted in mLB (1:100) was treated with the active flavonoids, incubated at 250 rpm for 24 h at 30 °C, and centrifuged at 12,000 rpm for 15 min. Supernatants (75 μL) were added to 125 μL of 2 % azocasein and incubated without agitation for 30 min at 37 °C. Thereafter, 600 μL of TCA (trichloroacetic acid solution - 10%) was added to terminate proteolysis. The reaction mixture was cooled at −20 °C for 30 min to precipitate the unreacted azocasein, which was separated by centrifugation at 12,000 rpm for 10 min. Supernatants (600 μL) were mixed with 700 μL of 1 M sodium hydroxide, and absorbances taken at 440 nm [34].

2.5.6. Thermostable direct hemolysin (TDH) production

Hemolysin inhibition was determined as previously described with some modification [35]. Briefly, *V. parahaemolyticus* in 2 mL of mLB (1:100) were incubated with or without the active flavonoids at 250 rpm for 24 h at 30 °C. The sheep blood was prepared by centrifuging at 3000 rpm and 4 °C to obtain erythrocytes, which were washed and adjusted with PBS to 5 % (v/v). Following incubation, the culture optical densities were measured at 600 nm and the *V. parahaemolyticus* cells (500 μL) were aliquoted into 2 mL of freshly prepared 5 % sheep blood, incubated for 5 h at 37 °C, and centrifuged at 8000 rpm for 10 min. Supernatant absorbances were measured at 570 nm using a UV spectrophotometer. Controls were prepared by adding PBS and derivatives to the erythrocytes.

2.5.7. Siderophore production

The effects of the derivatives on siderophore production was assessed using a Chrome Azurol Sulfonate (CAS) blue agar assay, as previously described with slight adjustment [36]. Briefly, CAS (60.5 mg) dissolved in 50 mL H_2O was added to 10 mL of iron (III) chloride solution (1 mM $FeCl_36H_2O$, 10 mM HCl) and stirred slowly, and then a solution containing 72.9 mg of HDTMA in 40 mL H_2O was added. The resulting dark blue solution was autoclaved at 121 °C for 15 min. Simultaneously, agar medium containing 20 g agar, 25 g LB, 20 g NaCl, and 1000 mL of H_2O was also autoclaved. After cooling to 45–50 °C, different concentrations of the flavonoids were introduced into the agar medium and subsequently, the CAS/iron (III)/HDTMA complex solution equivalent to 10 % of the media was added carefully along the flask side wall with stirring to avoid bubble formation. The resulting blue agar medium was aliquoted in petri-dishes (20 mL), dried, and centrally inoculated with 10 μL of 24 h culture inoculum and incubated for 5 days at 30 °C. Orange haloes around colonies represented siderophore (an iron chelator) production. All glassware used was cleaned with 35 % 6 M HCl, rinsed with dH_2O, and dried before use.

2.6. Isolation of RNA and quantitative real time-polymerase chain reaction (qRT-PCR)

V. parahaemolyticus culture was diluted in a 25 mL flask containing mLB (1:100), grown to OD 1.0 at 250 rpm and 30 °C, and incubated with 20 μg/mL with or without the active flavonoid derivatives for 3 h. RNase solution (700 μL; RNAlater, Ambion, TX, United States) was added to prevent degradation, cells were pelleted at 13,000 rpm for 5 min at 4 °C, and supernatants were discarded. Total RNA from the pellet was

obtained using RNeasy Mini Kits (Valencia, CA, United States), while RNA purity and quantity (ng/μL) were determined using a Nanodrop spectrophotometer (GE, Chicago, IL, United States). qRT-PCR was used to assess the expressions of 24 biofilm, virulence, membrane, hemolysin, and motility-related genes. Gene primers and their respective sequences are available in Table S2 qRT-PCR was conducted using the ABI StepOne Real-Time PCR system (Applied Biosystems, Foster City, CA, United States) and Power SYBR® Green master mix kit (Thermo Fisher, Warrington, UK). *16SrRNA* served as the reference gene [37]. The cycle threshold values (Ct) for the genes were generated and $2^{-\Delta\Delta CT}$ was employed to determine the relative gene expression level.

2.7. Applications of the flavonoids in food models

Litopenaeus vannamei, a type of shrimp, was purchased from a supermarket in Gyeongsan, Korea, and processed as previously described [33]. Shrimps were inoculated with *V. parahaemolyticus* by submersion in mLB containing the bacterial suspension (1:100) for 10 min to reach ~6 $\log_{10}$ CFU/g. The inoculated shrimps were dried for 45 min in a biosafety cabinet and immersed for 5 min in mLB containing the active derivatives at various concentrations or immersed in mLB or mLB with 20 μg/mL of STPP as a positive control. Treated shrimps were then placed in sterile bags, labeled, and refrigerated at 4 °C for 8 days. Samples were taken every two days, homogenized, serially diluted in PBS, and plated on mLB agar. *Vibrio* colonies were counted and expressed as $\log_{10}$ CFU/g [38].

In addition, fresh squids (Gyeongsan, Korea) were processed as previously described [33]. After drying for 1 h, squid pieces (2.5 cm × 2.5 cm) were placed in 6-well plates, inoculated with 3 mL of mLB containing *V. parahaemolyticus* (~10^6 CFU/mL), and incubated statically for 24 h at 30 °C to induce biofilm formation. Squid pieces were rinsed with PBS to remove non-adherent cells and then incubated for 24 h at 30 °C with or without flavonoid derivatives. Pieces were then rinsed, stomached, bead vortexed to release the attached *Vibrio* cells, plated, colonies were counted and expressed as log CFU/cm^2.

2.8. Effects of flavone derivatives on other foodborne pathogens and dual biofilm interactions

The inhibitory concentrations and antibiofilm effects of the selected flavonoids on other food-related pathogens, viz. *V. harveyi*, *S. aureus,* and *S. typhi* were investigated as described in sub-section 2.3.1 with slightly different media and incubation conditions. Specifically, mLB and LB were used for *V. harveyi* and *S. aureus* and incubated at 30 °C and 37 °C respectively. For *S. typhi*, nutrient broth (NB; Difco, New Jersey, USA) supplemented with 0.025 % glucose and incubated for 24 h at 30 °C was optimal for biofilm formation. A dilution of 1:100 in their respective media was used for all three pathogens.

Also, the effect of the derivatives on mixed biofilm interaction involving *V. parahaemolyticus* 17802 – Vp and *S. aureus* 6538 - Sa was examined in LB:mLB (1:1 v/v), followed by addition of equal amount of bacteria inoculum. The inoculums with or without flavonoid derivatives were dispensed in 96-well plates and incubated for 24 h at 37 °C. Biofilm formations were quantified as determined in sub-section 2.3.1. Note that diluted Vp and Sa were also aliquoted in the wells as controls.

2.9. Nucleotide leakage determination

This assay was conducted as previously described with slight modifications [39]. Overnight *V. parahaemolyticus* cultures were washed twice in PBS (10 mM), re-suspended in the same buffer, adjusted to OD_{620} 0.4, and treated with appropriate concentrations of the flavonoids at 30 °C. Samples were taken at each time point (0, 2, 4, 8, and 12 h), centrifuged at 10,000 rpm for 10 min, supernatants were filtered with microporous membrane (0.22 μm) and the absorbances (OD_{260} nm) were measured using a Multiskan EX plate reader.

2.10. Cytotoxic effects in Caenorhabditis elegans and in-silico profiling

The cytotoxic effects of the flavonoid derivatives were evaluated using *C. elegans* strain *fer-1* as reported but with slight modification [40]. In brief, ~35 non-infected, synchronized adult worms in M9 buffer (KH_2PO_4 3 g; Na_2HPO_4 6 g; NaCl 5 g; 1 L dH_2O) supplemented with 1 M $MgSO_4$ were pipetted into 96-well plates with or without different concentrations of the derivatives. Then, the plates were incubated statically in the absence of *V. parahaemolyticus* for 7 days at 25 °C. Nematode viabilities were determined daily for movement using the iRiS™ digital cell imaging system (Logos Biosystems, Korea). The cytotoxicity was expressed using Kaplan-Meier survival plots [41].

The physicochemical, toxicity and drug-likeness parameters of the derivatives were evaluated *in-silico* using PreADMET (https://preadmet.qsarhub.com/adme/), Molinspiration (https://www.molinspiration.com/), GUSAR (http://www.way2drug.com/gusar/acutoxpredict.html), and SwissADME (http://www.swissadme.ch/index.php) [42]. All were accessed on the May 3, 2023.

2.11. Data analysis

All assays were carried out in triplicate using at least two independent cultures. The analysis was conducted using the student's *t*-test. Results are presented as means ± SDs, and statistical significance was accepted for p values < 0.05. Graphs were plotted using SigmaPlot 14.0.

3. Results and discussion

3.1. Antibiofilm activities and MICs of the flavonoid derivatives against V. parahaemolyticus

The abilities of the 16 flavonoids to inhibit *V. parahaemolyticus* biofilm formation were initially evaluated at 20 and 100 μg/mL to obtain derivatives with high antibiofilm activities at lower concentrations (Table S1). Of the derivatives, 6-aminoflavone (6-AF), 3,2-dihydroxyflavone (3,2-DHF), and 2,2-dihydroxy-4-methoxybenzone (DHMB) exhibited the strongest biofilm inhibitory effects with 92, 99, and 98 % inhibition at 20 μg/mL and 96, 99, and 99 % at 100 μg/mL respectively. Others including 7-hydroxyflavone, fisetin, genistein, flavone, and phloretin inhibited biofilm formation by 54, 99, 63, 65 and 100 % at 100 μg/mL. Due to the antibiofilm potencies at lower doses, 6-AF, 3,2-DHF, and DHMB were selected for further investigation while flavone served as the scaffold control (Fig. 1A).

Furthermore, MIC as a key indicator of antibacterial activity revealed that 3,2-DHF, DHMB, phloretin, and flavanone inhibited *V. parahaemolyticus* at 20, 50, 50, and 100 μg/mL, respectively attributing their antibiofilm activities to the inhibitory effects on planktonic cell growth (Table S1). This agrees with a previous study where prenylated flavonoids showed antibacterial activity against *V. vulnificus* [43]. Conversely, biofilm inhibitor - 6-AF could not inhibit planktonic cell growth even at 250 μg/mL, suggesting a behavior typical of antibiofilm agents and could limit the risk of selective pressure mediated resistance. Our result corroborates findings that 6-AF reduced biofilm formation by *E. coli* [44] but promoted biofilm formation by *A. baumannii* [16] and this might be associated with the difference in their outer membrane compositions or doses applied. Our results indicate the potential of the derivatives to prevent the pathogen from initiating biofilm formation which could be due to possible interference with the biosynthesis of quorum sensing signals responsible for its formation.

The efficacies of 6-AF, 3,2-DHF, and DHMB were also compared with sodium tripolyphosphate (STPP), tetracycline (TET), and sodium hypochlorite (NaOCl), which are food-grade compound, an antibiotic, and disinfectant, respectively, used for microbial control (Fig. 1B). STPP with European food additive number E451(i) dose-dependently inhibited *Vibrio* biofilm formation by 94 % at 8 mg/mL, which was less

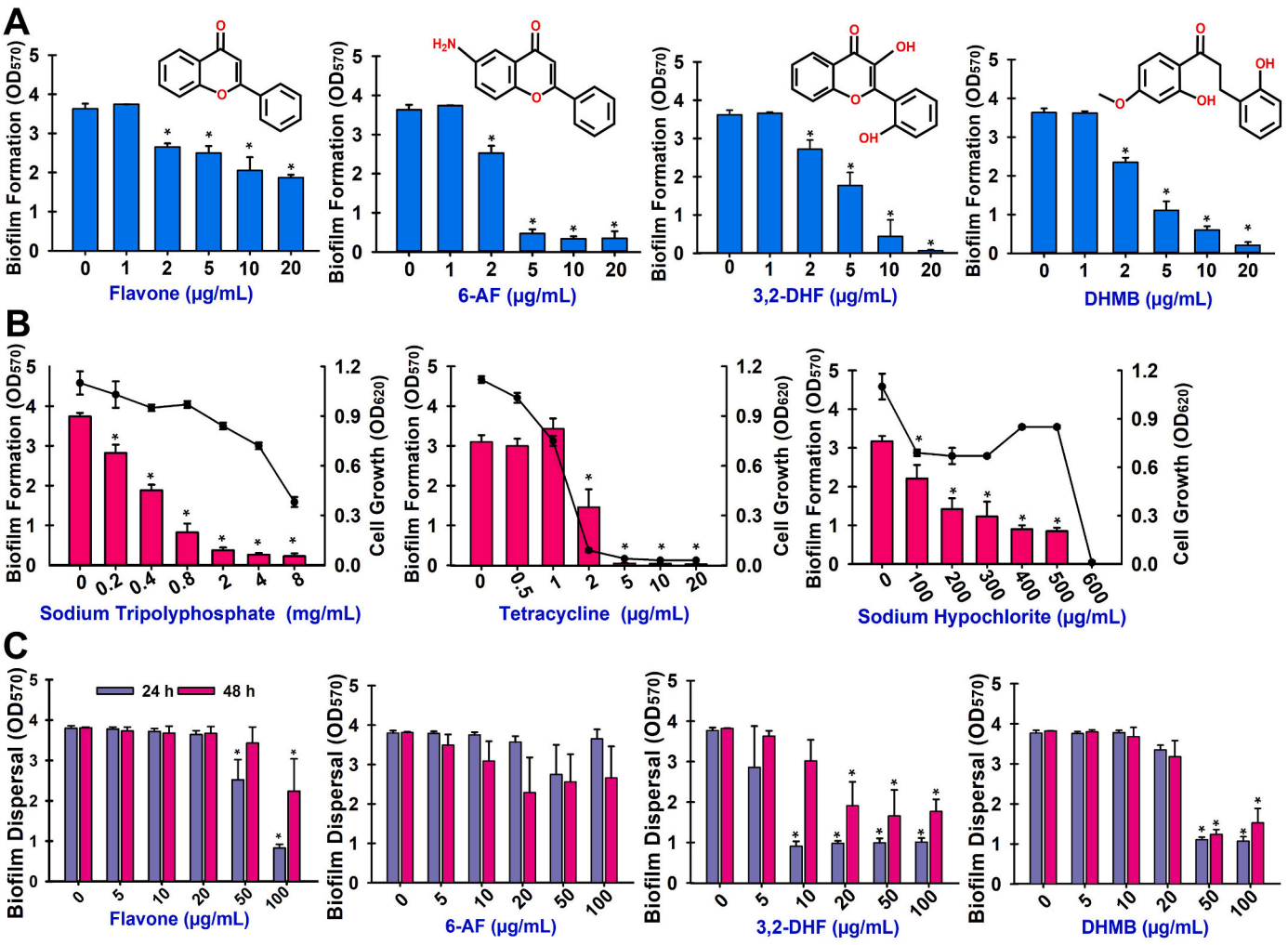

Fig. 1. Antibiofilm effects of flavonoid derivatives. The antibiofilm activities of the three active derivatives and the parent flavone at sub-MIC concentrations against *V. parahaemolyticus* **(A)**, comparison with three standard controls **(B)** and the biofilm disrupting effects of the flavonoids **(C)**. Bars represent biofilm formation and lines, the planktonic cell growth. * Denotes a significant difference at $p < 0.05$.

effective than 6-AF, 3,2-DHF and DHMB, with 90–98 % biofilm inhibition at 20 μg/mL. Also, TET and NaOCl at 20 and 600 μg/mL inhibited biofilm formation by 99 and 100 % respectively and was comparable to 3,2-DHF (98 %) at the same dose. These results suggest 3,2-DHF as a potent and suitable alternative for controlling *Vibrio* biofilms.

Furthermore, the biofilm age is believed to be largely responsible for the difficulties experienced in eradicating biofilms. Thus, we investigated the abilities of the three selected derivatives to disrupt 24 and 48 h old biofilms. As was expected, 24 h old biofilms were more easily disrupted than 48 h biofilms (Fig. 1C). For instance, flavone and DHMB at 100 μg/mL eradicated 24 h biofilms by 72–78 % but only achieved 41–60 % eradication of 48 h biofilms. Similarly, 3,2-DHF had a notably greater effect on 24 h biofilms (74 %) than 48 h biofilms (> 50 %) at only 20 μg/mL. Additionally, 3,2-DHF and DHMB at 5–20 μg/mL eradicated 24 h biofilms on polyethylene material, which is commonly used in food processing environments (Fig. S1). The biofilm-disrupting properties of 3,2-DHF and DHMB suggest their use for effective eradication of *Vibrio* biofilms from food contact surfaces. These observation is in line with a recommendation that new controls should possess extra attributes, such as biofilm inhibitory properties, to control bacterial pathogens more efficiently [45].

3.2. Microscopic and metabolic studies of antibiofilm activities

Here, microscopic methods determined the effects of flavonoid analogues on *V. parahaemolyticus* biofilms and morphology (Fig. 2). The 3D color-coded microscopic images showed enormous biofilm biomass in the untreated group with slight reductions upon treatment with 2 μg/mL of 6-AF, 3,2-DHF and DHMB while the biofilm biomass was notably reduced at 20 μg/mL (Fig. 2A). SEM showed that untreated control biofilms were composed of highly clustered cells that appeared to form microcolonies, and was inhibited by 6-AF, 3,2-DHF, and DHMB at 20 μg/mL as evident by the absence or marked reductions in cell aggregations (Fig. 2B). Interestingly, treatment with 6-AF induced cell elongation (5.4 ± 1.3 μm vs. 1.6 ± 0.3 μm for untreated controls) (Fig. S2A), which suggests interference with the bacterial divisome and agrees with a previous report that morin dose-dependently elongated *V. cholerae* cells [17]. Evidence of cell disruption characterized by pits and shrinkage were also observed in 3,2-DHF treated groups (Fig. 2Bix), indicating it targeted the cell membrane for antibacterial activities.

Furthermore, we examined whether 6-AF, 3,2-DHF, and DHMB interfered with the metabolic activities of biofilm cells (Fig. 2C). The TTC assay revealed that these derivatives reduced metabolic activity by 77–93 %, 90–98 %, and 98–99 %, respectively, at concentrations of 2–20 μg/mL, indicating 6-AF, 3,2-DHF, and DHMB-induced biofilm inhibitions were due to the suppression of metabolic activity.

3.3. Effects of flavonoid derivatives on growth kinetics

We monitored the effects of 6-AF, 3,2-DHF, and DHMB on the growth

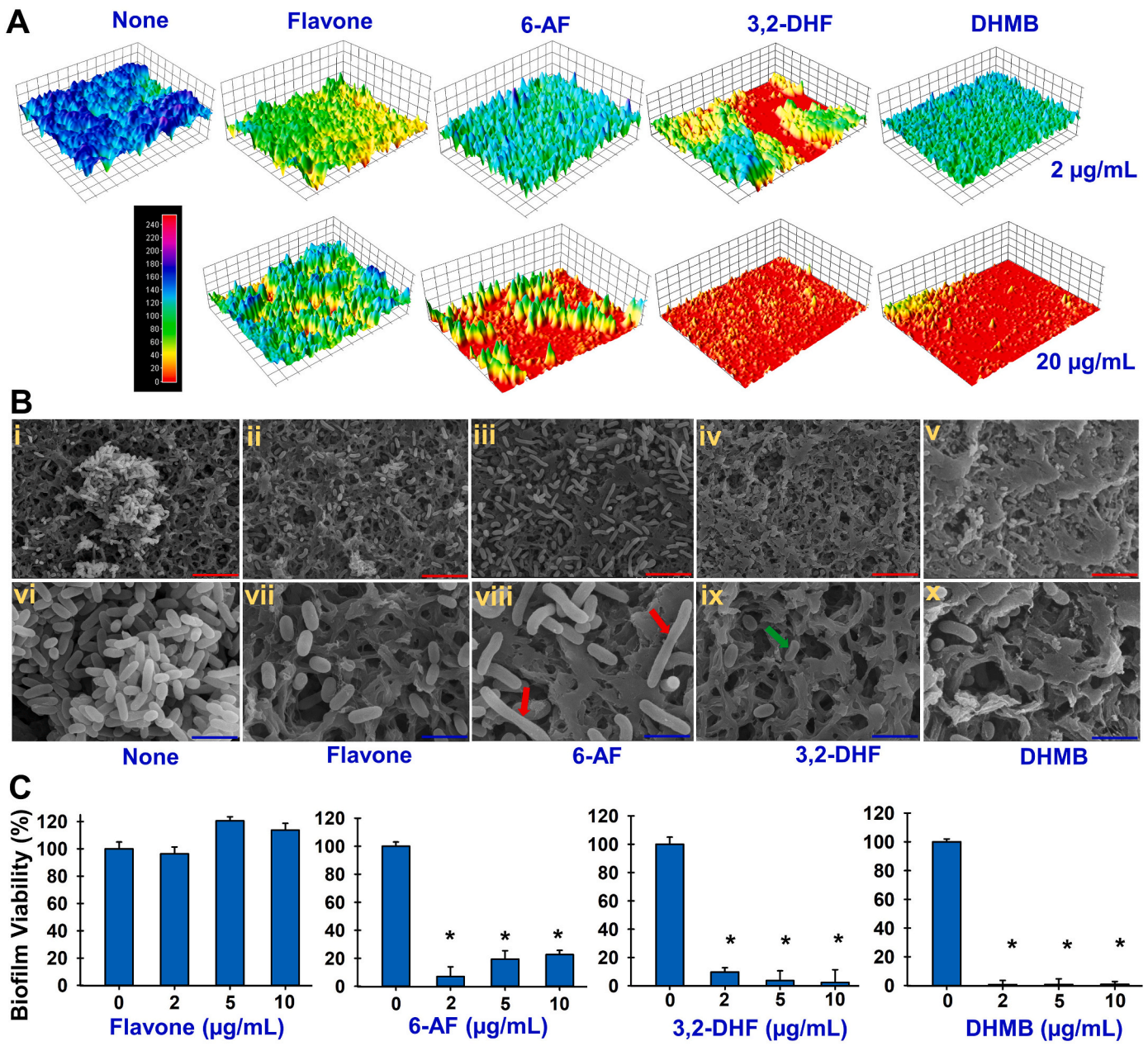

Fig. 2. Visualization of the antibiofilm activities of the flavonoids. Phase contrast microscope 3D images (**A**) and SEM images of flavonoid treated cells (**B**), effects of the analogues on biofilm metabolic activities **(C).** * Represents a significant difference ($p < 0.05$). Red and green arrows represent elongated and disrupted cells, respectively. Red and blue bars represent 10 and 5 μm, respectively.

of *V. parahaemolyticus* (Figs. S2B–E). Flavone at 2–20 μg/mL had a non-significant inhibitory effect on cell growth, whereas 6-AF did not affect cell growth. Notably, 3,2-DHF and DHMB retarded planktonic cell growth at 5–10 μg/mL with total inhibition at 20 μg/mL. Time kill studies were used to determine the killing rates of the derivatives (Fig. 3A). 3,2-DHF at 2 × MIC (40 μg/mL) was bactericidal to *V. parahaemolyticus* at log and stationary phases within 1 and 4 h, respectively, while DHMB became bactericidal after 12 and 24 h, respectively. Both showed growth phase-dependent activities, and log phase cells were more susceptible to 3,2-DHF and DHMB (100 μg/mL) than non-replicating cells at the stationary phase. Our observations were confirmed using PBS, in which bacteria can survive for long periods without replication (Fig. 3B). Treatment of both growth phases with 3,2-DHF at 2 × MIC in PBS resulted in delayed activity as compared with treatment in mLB, suggesting these compounds better target actively dividing cells. Of note, 3,2-DHF and DHMB displayed significant bactericidal activities at 40 and 100 μg/mL which are 20 and 8 times more active than NaOCl (800 μg/mL) indicating potential application as surfactants or disinfectants.

3.4. Flavonoid derivatives inhibited adhesion factors and indole production

Central to the biofilm life cycle are adhesion factors involved in movement, colonization, polysaccharide production and dispersal and the dual flagellar system specifically in *V. parahaemolyticus* confers enormous advantage. To determine the effects of 6-AF, 3,2-DHF, and DHMB on *V. parahaemolyticus* virulence, we investigated their effects on adhesion factors, viz. motility, cell surface hydrophobicity (CSH), and auto-aggregation, which are critical for initial attachment and biofilm formation on surfaces. Relative to the untreated control (Fig. 3C and D), 6-AF and DHMB substantially restricted flagella-mediated swimming

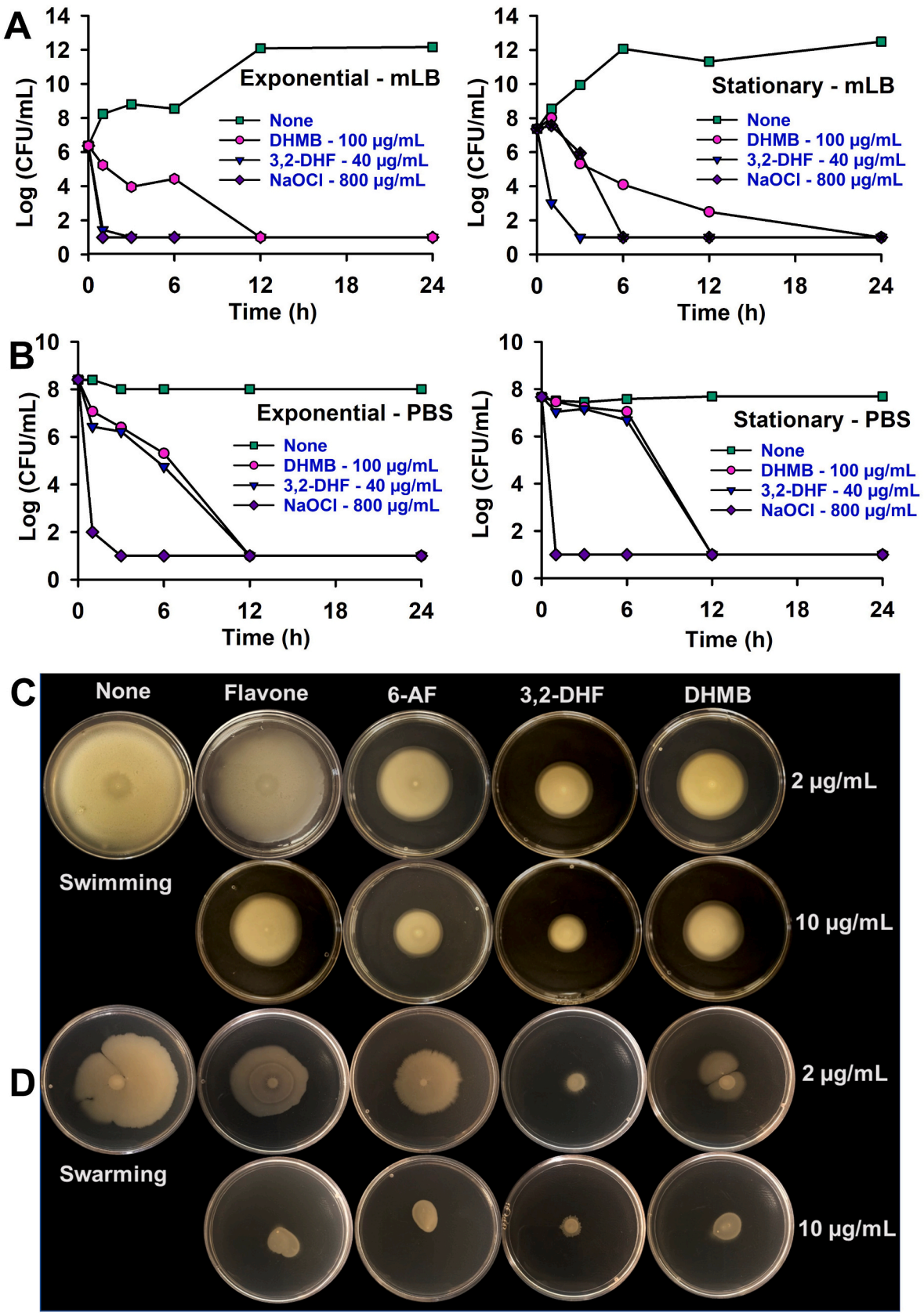

Fig. 3. Effects of active flavonoids on *V. parahaemolyticus* survival and motility. Time killing effects of flavonoids against *Vibrio* exponential and stationary growth phases in mLB **(A)**, PBS **(B)**, and their effects on *Vibrio* swimming **(C)** and swarming motilities **(D)**. * Represents a significant difference ($p < 0.05$). Exponential and stationary phase cells were obtained by culturing for 3 h and 14 h at 30 °C and 250 rpm, respectively before use.

capacity by 44–60 % at a sub-MIC of 2 μg/mL and by 63 % at 10 μg/mL, whereas lateral flagella-mediated swarming was suppressed at 2 and 10 μg/mL by 53–56 % and 72–76 %, respectively (Figs. S3A and B). Our finding corroborates reports that punicalagin suppressed motility and related genes in *V. parahaemolyticus* [30]. The motility inhibition by the derivatives shows the capacity to restrict movement on surfaces and attenuate flagella biosynthesis, bacterial adherence and disrupt effector protein delivery [46].

Most food contact materials, including stainless steel, plastic, and rubber, are hydrophobic and easily colonized by hydrophobic pathogens like *V. parahaemolyticus*. 3,2-DHF totally inhibited its cell surface hydrophobicity (CSH) at 2–10 μg/mL, and flavone achieved a 64–87 % reduction while DHMB and 6-AF inhibited CSH by 11–49 % and 31–41 %, respectively (Fig. 4A). In this study, CSH inhibition could partially explain the mechanism of biofilm inhibition by preventing surface colonization. Also, it could minimize food spoilage by limiting interactions between the bacteria and nutritious hydrophobic food components such as proteins and oils.

Recently, the upregulation of certain proteins - TraA, LysR and OmpA was reported to promote autoaggregation and confer survival on *V. parahaemolyticus* [47]. It has the ability to auto-aggregate (Fig. 2Bvi), and can form cell clusters essential for adhesion and biofilm formation [48]. Hence, the effect on autoaggregation was examined and notably at 2 μg/mL, 3,2-DHF inhibited auto-aggregation by 84 % with complete inhibition at higher doses (Fig. 4B). The effect of DHMB (67–75 %) was similar to that of flavone (70–76 %) at 5–10 μg/mL and better than 6-AF (65 % inhibition at 10 μg/mL). The inhibition of auto-aggregation particularly by 3,2-DHF suggests it could disrupt *Vibrio* surface proteins (autoagglutinins) such as flagella, and type IV pili or modify their interaction sites. This observation further supports the biofilm inhibitory mechanism.

Vibrio produces indoles (signaling molecules) from tryptophan using tryptophanase (TnaA), which plays notable roles in quorum sensing (QS), virulence, antibiotic resistance, bacterial homeostasis, and biofilm formation [49,50]. In this study, 6-AF reduced extracellular indole levels by 58, 64, and 74 % at 2, 5, and 10 μg/mL, respectively, while 3,2-DHF and DHMB reduced indole levels by 87–90 % and 58–71 %, respectively, at 2–5 μg/mL and eliminated it at 10 μg/mL (Fig. 4C). Being a signaling molecule, its inhibition corroborates the antibiofilm and antivirulence activities of 6-AF, 3,2-DHF, and DHMB and also indicates their potential as quorum quenchers.

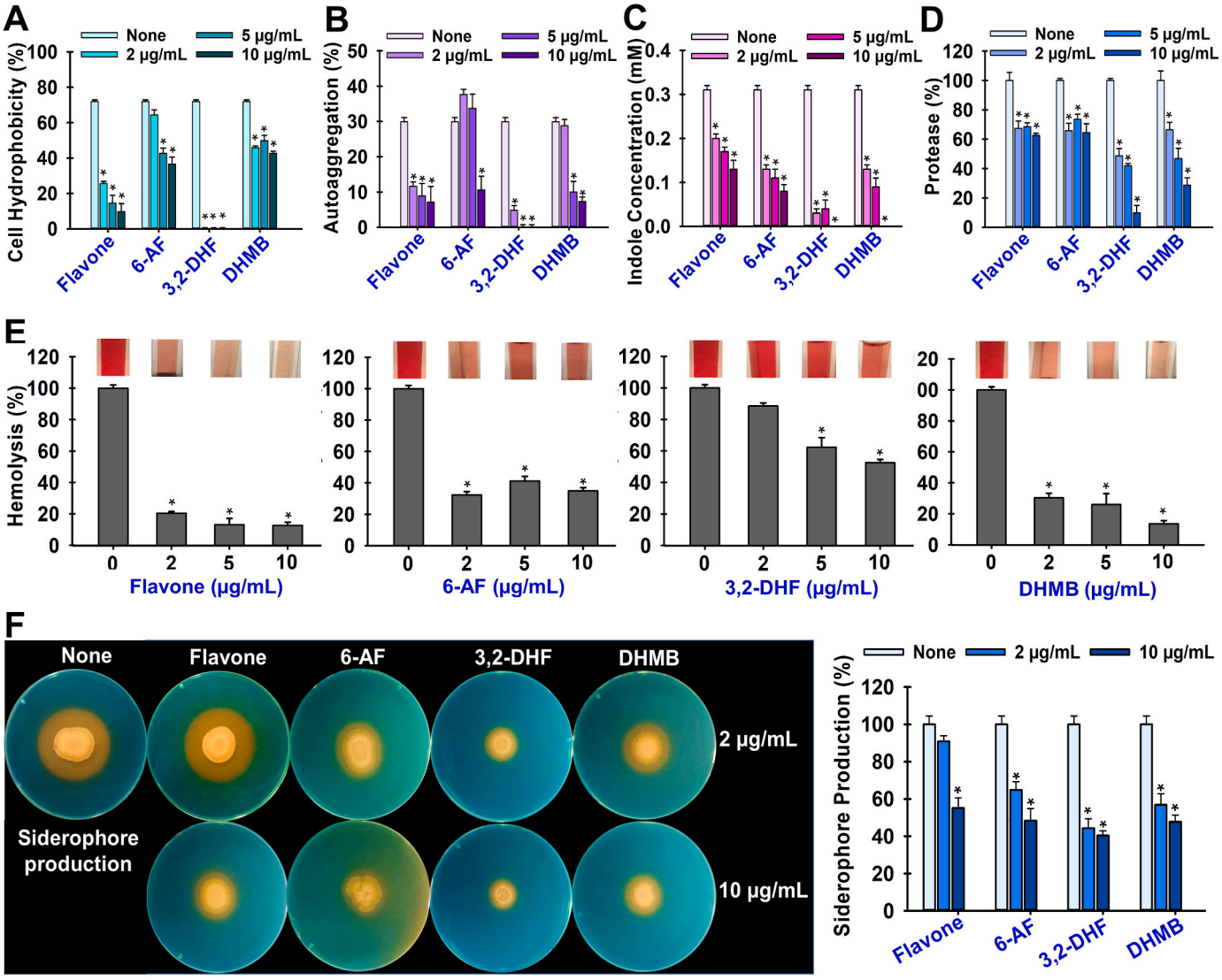

Fig. 4. The effects of flavonoid derivatives on adhesion and virulence factors. Cell surface hydrophobicity **(A)**, autoaggregation **(B)**, extracellular indole **(C)**, protease production **(D)**, hemolysin **(E)** and siderophore production **(F)** in *V. parahaemolyticus*. *Represents a significant difference ($p < 0.05$).

3.5. Inhibition of virulence factors by the flavonoids

Vibrio spp. proteases are reportedly pathogenic to prawn and the shrimp filtrates containing *Vibrio* exoenzymes caused kidney and liver damage and death in mice [51,52]. Hence, we studied the effect of derivatives on *Vibrio* proteases and at 2–10 μg/mL, flavone inhibited protease production (33–37 %) in the same manner as 6-AF (34–36 %), while 3,2-DHF (51–90 %) displayed better activity than 6-AF and DHMB (34–71 %) (Fig. 4D). Protease inhibition by these derivatives explains their abilities to control the pathogenicity and the cytotoxicity of *V. parahaemolyticus*.

In addition, the thermostable direct hemolysin (TDH) is a critical

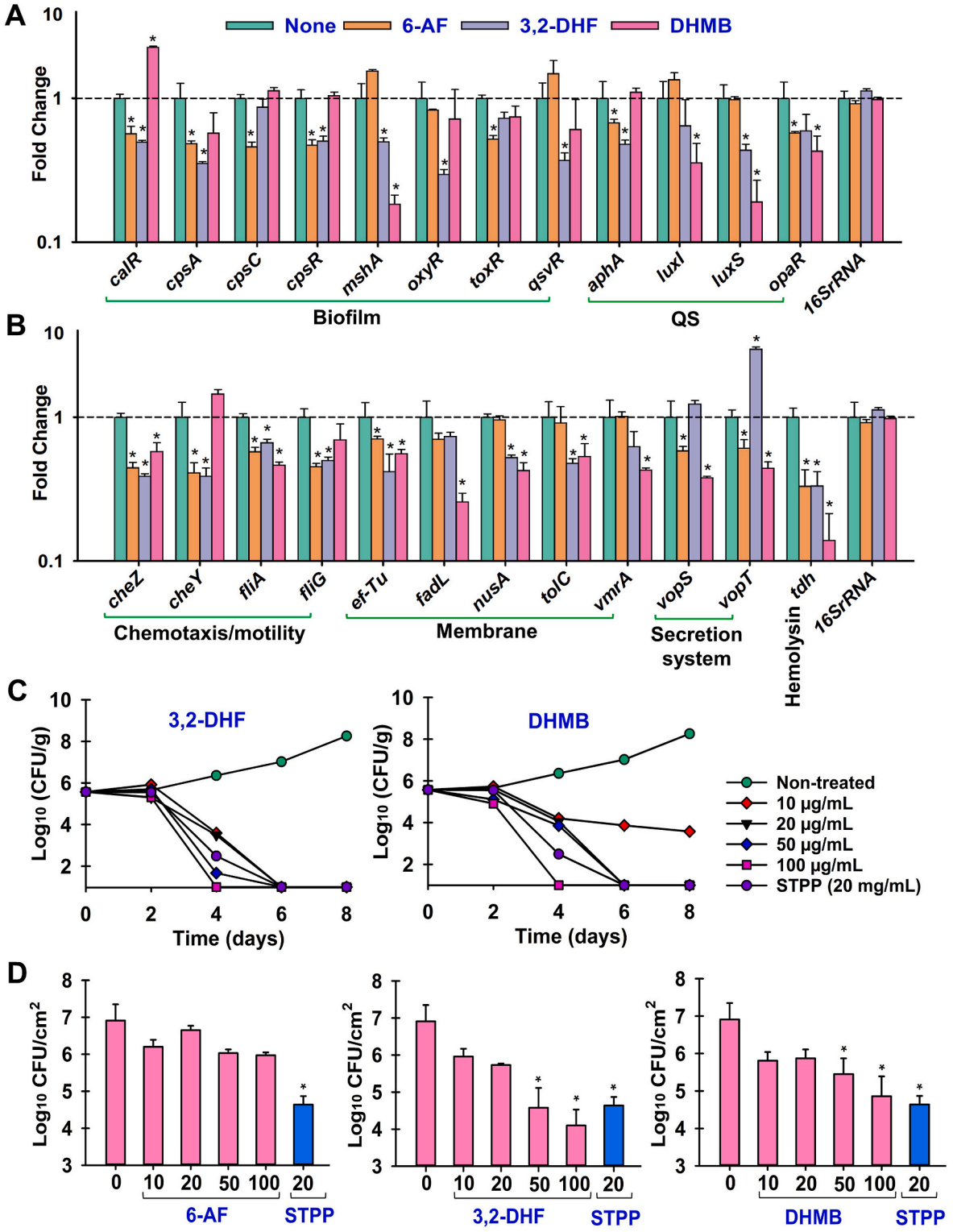

Fig. 5. Effects of flavonoid derivatives on gene expression and seafood preservation. Relative gene expression analysis of *Vibrio* cells treated with 20 μg/mL of 6-AF, 3,2-DHF, and DHMB **(A-B),** antibacterial effects of the three derivatives on shrimps inoculated with *V. parahaemolyticus* **(C),** and biofilm eradication effects on squid **(D).** * Denotes a significant difference ($p < 0.05$). Sodium tripolyphosphate (STPP) served as the control.

pandemic marker found in the pathogenic strains of *V. parahaemolyticus*. Apart from seafoods, the bacterium can produce hemolysin in non-seafood products such as chicken, pork, and egg fried rice [53]. In this study, 6-AF, 3,2-DHF, DHMB, and flavone inhibited hemolysin production (Fig. 4E). Specifically, flavone and DHMB at 2–10 μg/mL significantly inhibited TDH production by 80–87 % and 70–86 % respectively. Interestingly, 6-AF inhibited hemolysin production more than 3,2-DHF (65–68 % *vs*. 16–47 %). This agrees with a previous study which found that 7,8-DHF inhibited *S. aureus* α-hemolysis by inhibiting *hla* gene expression [54]. Furthermore, hemolysin production in *V. parahaemolyticus* is directly correlated with biofilm formation and regulated by ToxR protein [12]. Therefore, TDH inhibition suggests the flavonoids' ability to attenuate biofilm formation, enterotoxicity, cytotoxicity, and erythrocyte lysis that characterize *Vibrio* colonization or ingestion. Notably, 6-AF, 3,2-DHF, and DHMB were non-toxic to human blood (Fig. S3C), indicating that the observed hemolytic activity was induced by *V. parahaemolyticus*.

V. parahaemolyticus deploys high affinity iron binding compounds called siderophore and specifically vibrioferrin for iron acquisition in the iron deficient niches. *Vibrio* requires bioavailable iron for growth, cellular redox processes, virulence activities, and survival in food and clinical environments [55]. Therefore, disrupting this acquisition system provides a strategy for controlling *Vibrio*. At 2 and 10 μg/mL, flavone, 6-AF, DHMB, and 3,2-DHF significantly restricted siderophore production by 61–63 %, 54–66 %, 60–66 %, and 69–72 % (Fig. 4F). The results reflect the capacity of the derivatives to limit the production and extracellular release of vibrioferrin. Consequently, apart from affecting *Vibrio* survival, this inhibition could disrupt the bacterial machinery responsible for producing virulence factors, such as collagenase and hemolysin.

3.6. Flavonoid derivatives repressed biofilm, QS, and hemolysin-related gene expressions

We examined the effects of 6-AF, 3,2-DHF, and DHMB on the expressions of 24 genes to decipher the molecular basis responsible for their antibiofilm and antivirulence activities (Fig. 5A and B). 3,2-DHF repressed the expressions of *cpsA, mshA, oxyR,* and *qsvR* (Fig. 5A), which are responsible for capsular polysaccharide synthesis, biofilm formation, surface attachment, and oxidative stress by 2.8-, 2.0-, 3.4-, and 2.7-fold respectively [56]. Similarly, 6-AF and DHMB downregulated *toxR* and *mshA* by 2.0- and 5.4-fold, respectively, while QS regulators - *aphA* and *opaR* associated with *Vibrio* response to virulence at low and high cell densities were repressed by 6-AF (1.5- and 1.7-fold, respectively) [57]. 3,2-DHF and DHMB downregulated the QS-related genes *luxS* and *opaR* by 2.3 and 1.7-fold and 5.2 and 2.3-fold, respectively (Fig. 5A). Also, 6-AF and 3,2-DHF suppressed the expressions of *fliG, cheZ,* and *cheY* (Fig. 5B), which control chemotaxis, flagellar biosynthesis, and clockwise and anticlockwise rotation [58]. Additionally, 6-AF, 3,2-DHF, and DHMB downregulated *tdh,* encoding hemolysin production in *V. parahaemolyticus*, by 3.0-, 3.0-, and 7.2-fold, respectively, and notably downregulated other genes relating to the membrane and effector secretion systems (Fig. 5B). The downregulation of various biofilm-, QS-, motility-, hemolysin-, and secretion system-related genes observed provides molecular evidence underlining various inhibitory effects of the flavonoids in this study.

3.7. Applications of flavonoid derivatives in food models

Vibrio causes necrotic disease and contaminates shrimp in aquacultures. Accordingly, shrimps were used to evaluate the antimicrobial activity of the derivatives in the food system. As shown in Fig. 5C, the untreated *Vibrio* population increased steadily from 5.6 $\log_{10}$ CFU/g to 8.6 $\log_{10}$ CFU/g after 8 days. STPP (the positive control) caused a 3.1 log CFU/g reduction, which was better than 3,2-DHF or DHMB with 1.5 and 2.1 log CFU/g reductions at 20 μg/mL, but less active than 3,2-DHF (3.9 log CFU/g) at 50 μg/mL after 4 days. Notably, 3,2-DHF and DHMB at 100 μg/mL inhibited the bacterial population to below the detection limit on the 4th day. Interestingly, shrimps' appearance remains intact with visual observation but retains the yellow color of 3,2-DHF (data not shown). These results suggest that 3,2-DHF and DHMB are capable of inactivating or killing *Vibrio* on seafood surfaces and might be suitable as additives for long-term seafood storage. Invariably, they could reduce the viability of foodborne pathogens to prevent the quorum needed for biofilm initiation.

Similarly, the flavonoids also displayed biofilm dispersing effects in a food matrix (Fig. 5D). Biofilm formation on untreated squid (6.9 $\log_{10}$ CFU/cm^2) was slightly reduced by ~1 log CFU/cm^2 with 3,2-DHF and DHMB treatment at 20 μg/mL after 24 h. Interestingly, 3,2-DHF at 100 μg/mL dispersed the biofilm by 2.8 log CFU/cm^2 which was better than 2.3 and 2.1 log CFU/cm^2 for DHMB and STPP (20 mg/mL) respectively. Overall, 3,2-DHF was more potent against *V. parahaemolyticus* than DHMB or STPP in food matrices and its application as a food grade chemical is further supported by the role played in proliferating the muscle stem cells of porcine during cultured meat production [59]. Of note, antibiofilm activity was more pronounced on polyethylene material (Fig. 1A and S1) than on squid (Fig. 5D) and could be explained by the high nutritional content of squid which conferred some resistance to the preformed biofilm cells.

3.8. Flavonoid derivatives inhibited other foodborne pathogens and their mixed biofilm formation

We investigated the efficacy of the active derivatives against biofilm formation of other important foodborne pathogens. *V. harveyi* which is notorious for vibriosis and biofilm formation in aquacultures was dose-dependently inhibited by 3,2DHF and DHMB with MIC values of 20 and 50 μg/mL respectively, while 6-AF only inhibited biofilm as in *V. parahaemolyticus* (Fig. 6A). In addition, *S. aureus* contaminates commercial food products and is associated with medically important biofilms and food poisoning. Its biofilm formation was inhibited by 100 and 50 % at 50 μg/mL in the 3,2-DHF and DHMB treated groups respectively while 6-AF had no antibiofilm effects (Fig. 6B). Similarly, *Salmonella* spp., known to form biofilms on surfaces in slaughterhouses and food processing factories, was totally inhibited by 6-AF and 3,2-DHF at their MICs of 5 and 2 μg/mL, respectively. Also, DHMB inhibited *Salmonella* biofilm formation and had MIC value of 200 μg/mL (Fig. 6C). The results suggest that flavonoid derivatives, particularly 3,2-DHF possess broad-spectrum antibiofilm effects against other foodborne pathogens and can serve as their control. Notably, the antibacterial effect of 6-AF against *S. typhi* corroborates a previous report that *Mycobacterium tuberculosis* was inhibited by 7-aminoflavone [60]. Typically, aminoflavones possess one or more amino groups on the flavone nucleus, and it is believed that the locations of amine groups and type of bacterial isolates accounted for the differential effects.

Furthermore, mixed species rather than single biofilm are mostly responsible for biofilm contamination and its associated persistence and spoilage in the food industry. Hence, we envisaged and investigated the effects of 6-AF, 3,2-DHF, and DHMB on mixed biofilm formation of *V. parahaemolyticus* and *S. aureus*. Notably, both 3,2-DHF and DHMB from 5 μg/mL significantly suppressed the mixed biofilm formation and as expected, 6-AF could only prevent *Vibrio* involvement in the biofilm interaction (Fig. 7A). SEM observation showed the presence of both pathogens in polymeric matrix (Fig. 7Bix) and their significant inhibition upon treatment with 50 μg/mL of 3,2-DHF and DHMB (Fig. 7Bxi, xii). These results further support the broad-spectrum applications of the flavonoids for controlling multispecies biofilms in food production facilities. Again, 6-AF, 3,2-DHF and DHMB exhibited membrane shrinking effects (Fig. 7Bx, xi, xii) and subsequently, we examined the release of nucleic materials which reflects membrane damage (Fig. 8A). Relative to the untreated group, all the three flavonoids showed a significant release of nucleotides suggesting the membrane as target for

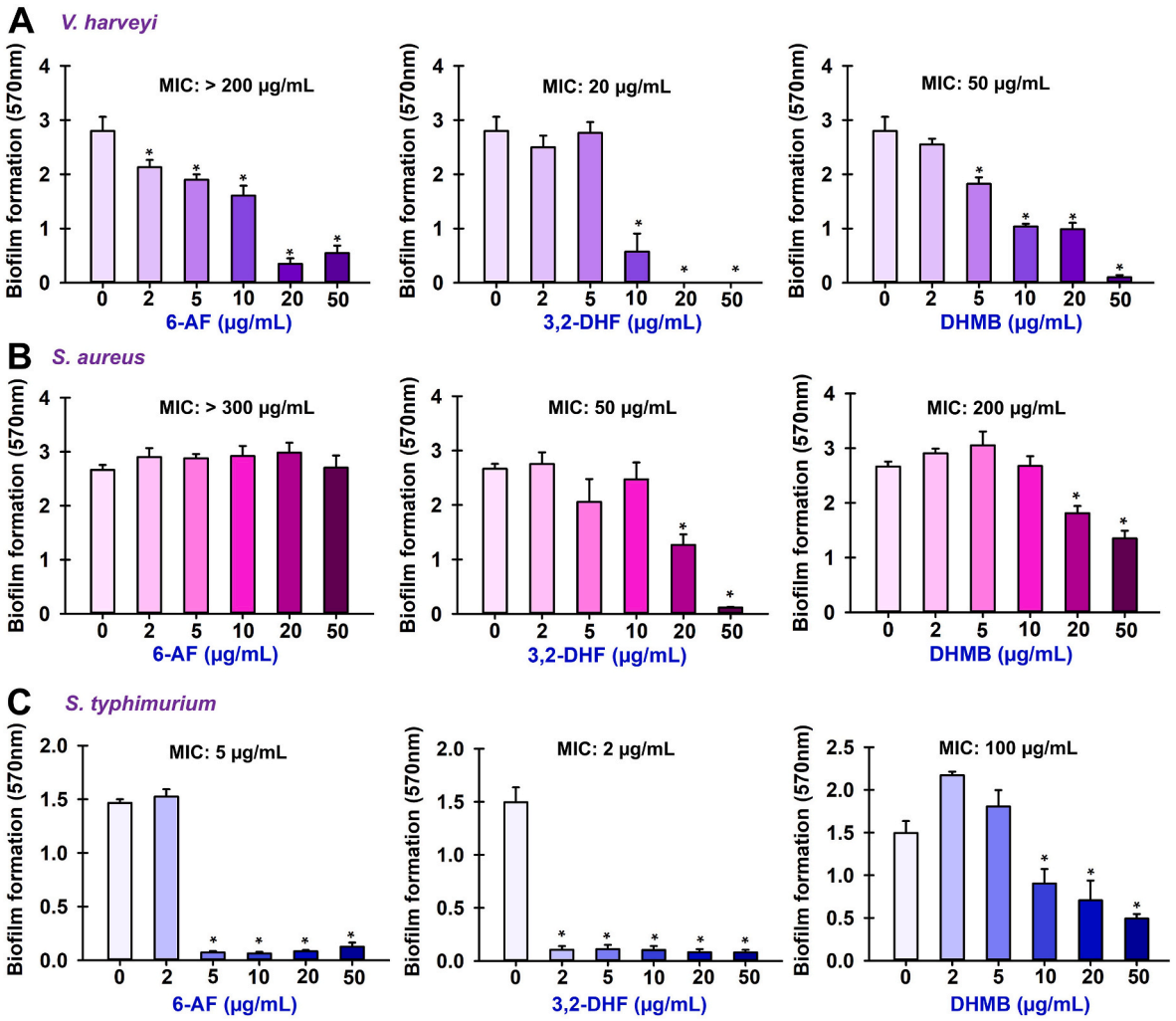

Fig. 6. The inhibitory effects of the three flavonoid derivatives against biofilm formation and planktonic cells of important food pathogens. *Represents a significant difference at $p < 0.05$.

antimicrobial activities.

3.9. Flavonoid derivatives displayed reasonable toxicity in-vivo and in-silico

New chemical entities must be non-toxic to be considered as candidates for food additives or therapeutics. Hence, the cytotoxic effects of 6-AF, 3,2-DHF, and DHMB were investigated *in-vivo* using a *C. elegans* model (Fig. 8B). 6-AF at 10–400 µg/mL did not significantly affect worm survival, which corroborates its effects on human epithelial (HeLa) and human breast cancer cells (MDA MB 435) [61]. Similarly, 3,2-DHF was non-toxic at MIC levels but mildly toxic to worms at 20 × MIC (400 µg/mL) (70 % survival rate after 7 days) (Fig. 8B). The observed non-toxic effects agree with the report of 7,8-DHF against lung epithelial cells [54] and phloretin which alleviated induced colitis in a rat model [44]. However, DHMB exhibited toxicity at 10 µg/mL, which increased in a concentration and time-dependent manner. Interestingly, benzophenones have been applied to food-contacting materials and used as food additives [62], and it has been reported they had no adverse effect on rats fed 20 mg/kg/day for 90 days, which is equivalent to 1200 mg/day for a 60 kg human [63].

Furthermore, the BOILED-Egg and bioavailability radar predictive models showed that 6-AF, 3,2-DHF, and DHMB have good physicochemical properties, excellent blood-brain barrier permeabilities and intestinal absorption rates (Fig. S4). Also, i*n-silico* ADME analysis (Table S3) showed all the three satisfied Lipinski's rule of five, Veber (GSK), Egan (Pharmacia), Muegge (Bayer), and Ghose parameters (Table S4). However, it also showed medium risk to hERG. Overall, the three compounds, particularly 6-AF and 3,2-DHF, showed reasonable drug-like properties. Nonetheless, further toxicity evaluations are required in more advanced models.

Of the three selected flavonoids, 3,2-DHF, a natural product, exhibited the most potent activity against *V. parahaemolyticus* planktonic cells, biofilm formation, virulence and other foodborne bacteria. We envisage that the presence of a hydroxyl group at the C3 position on the C-ring and at C2 on the B-ring of the flavone structure explains why 3,2-DHF had greater activity than parent flavone which lacks hydroxyl group. This supposition is supported by the finding that hydroxylation at these locations was found to be responsible for antifungal activity against *Saccharomyces cerevisiae* [23]. Its efficacies and the predicted safety in this study corroborate previous antioxidative, neuroprotective and stem cell proliferative activities in meat production [25,26,59]. Overall, the flavonoids showed strong antimicrobial activities and exhibited mechanisms of action ranging from cell membrane disruption to interference with metabolic activity, virulence, and cell division for the control of *Vibrio* infection (Fig. 9).

4. Conclusion

In the current study, 6-AF, 3,2-DHF, and DHMB were found active

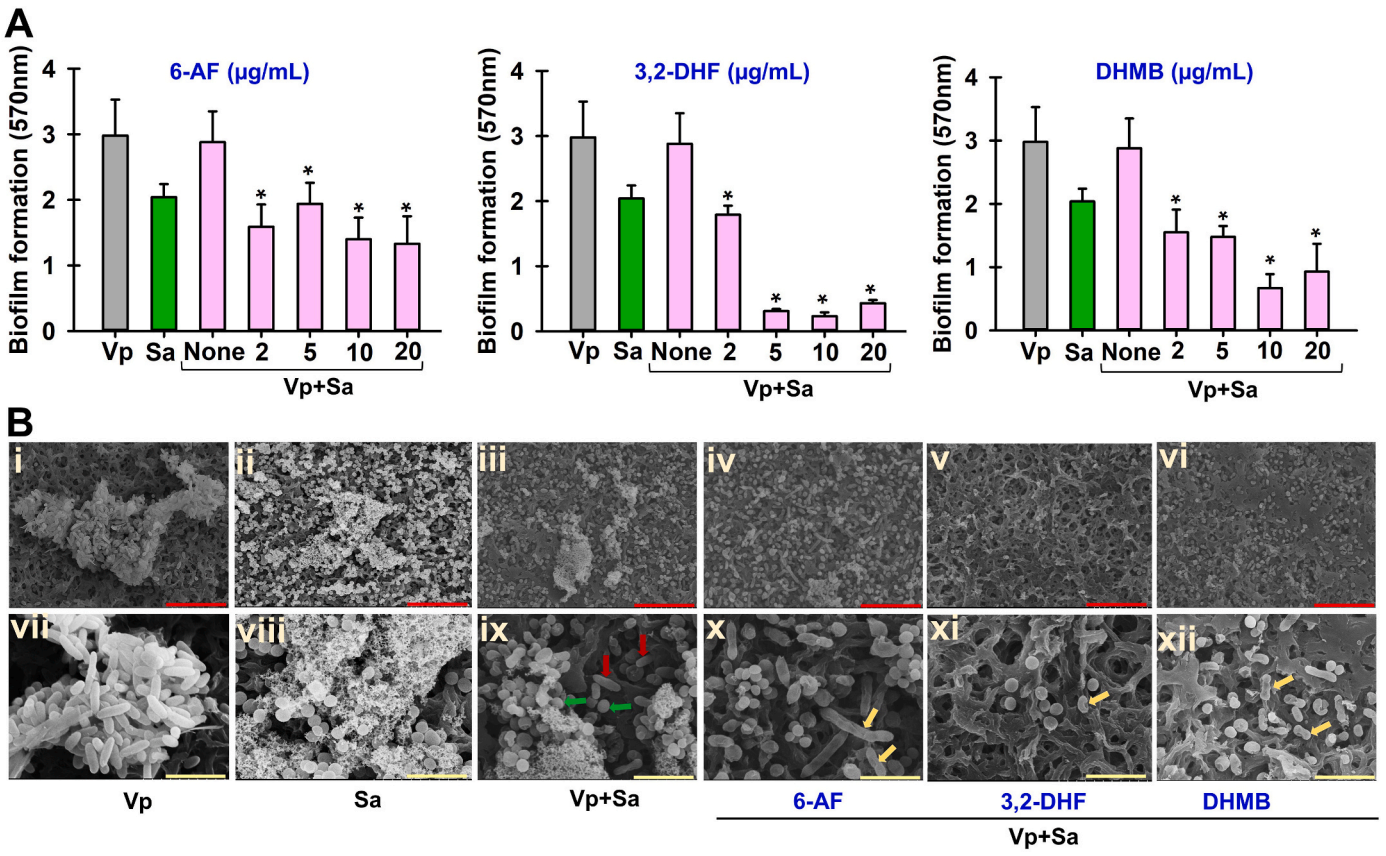

Fig. 7. The effects of flavonoid derivatives on mixed biofilm formation. The antibiofilm effects of 6-AF, 3,2-DHF, and DHMB against mixed *V. parahaemolyticus* - (Vp) and *S. aureus* – (Sa) biofilm formation **(A)**, SEM observation of the activities against mixed biofilm formation **(B)**. *Represents a significant difference ($p < 0.05$). The red and green arrows represent Vp and Sa while the yellow arrows indicate disrupted cells. Red and yellow bars represent 10 and 5 μm, respectively.

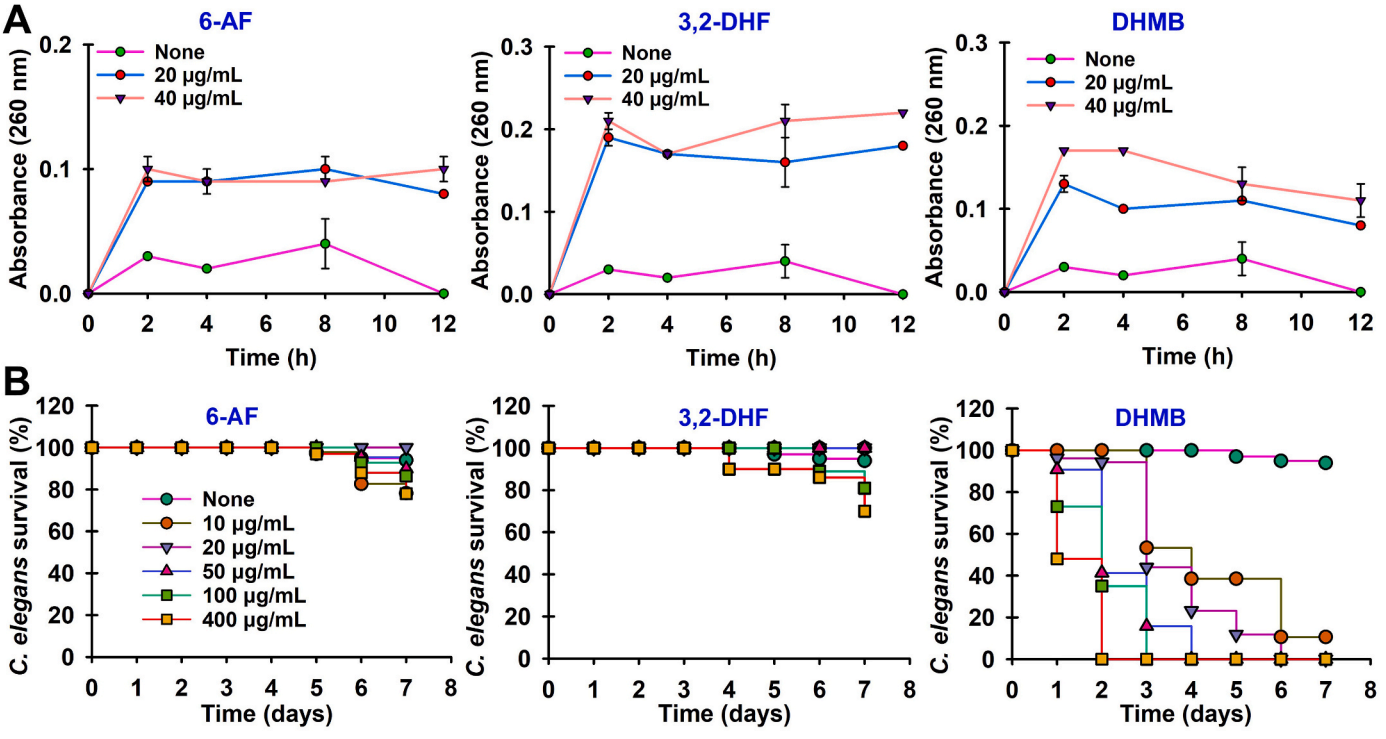

Fig. 8. Nucleotide leakages upon treatment with the derivatives **(A)**, and *in-vivo* cytotoxic studies of the active flavonoids in *C. elegans* **(B)**.

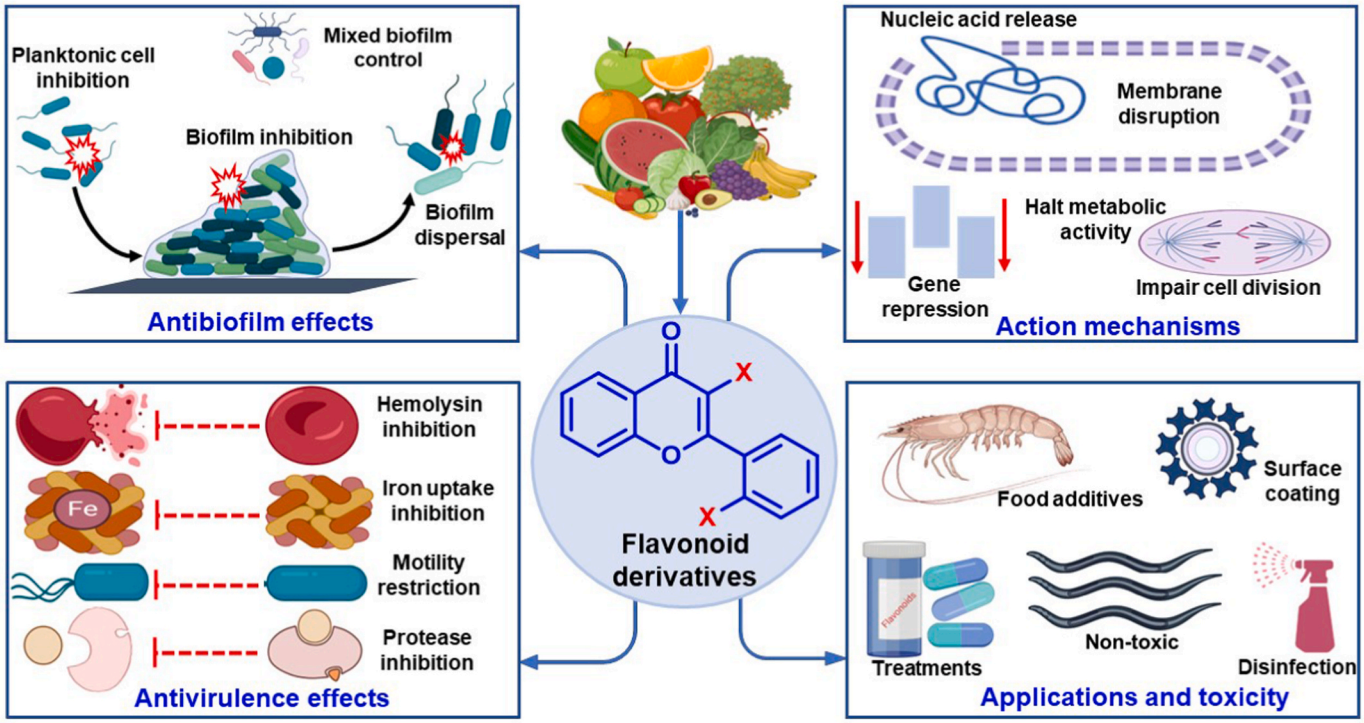

Fig. 9. A summary of various activities displayed by the flavonoid derivatives and their possible future applications.

against biofilm formation of *V. parahaemolyticus*. The three derivatives especially 3,2-DHF significantly attenuated adhesion factors and other virulence properties that aid surface colonization and pathogenicity. It showed a reasonable safety profile and limited the proliferation of *V. parahaemolyticus* in shrimp models as well as preserving their appearances. It disrupted mixed species biofilm formation including *S. aureus* and exhibited antimicrobial properties better than sodium tripolyphosphate currently used as food additive (E451i). Importantly, the flavonoids demonstrated antimicrobial activities by interfering with the biofilm metabolic activity, cell division and membrane integrity. Taken together, this study for the first time discovered some flavonoid derivatives, particularly 3,2-DHF as a potential multifunctional bioactive compound capable of ensuring safety against *V. parahaemolyticus* and *V. harveyi*. Since this study used reference strains, food isolates and clinical isolates would be further investigated. The flavonoids can also be leveraged for application in surface coatings, active packaging materials, and cleaning of contact materials. However, to ensure translation into food or clinical application, further sensory and toxicity assessments in advanced models are recommended.

CRediT authorship contribution statement

Olajide Sunday Faleye: Investigation, Methodology, Data curation, Formal analysis, Software, Visualization, Writing – original draft. **Jin-Hyung Lee:** Conceptualization, Writing – review & editing, Project administration, Funding acquisition, Resources. **Jintae Lee:** Conceptualization, Writing – review & editing, Project administration, Funding acquisition, Resources.

Declaration of competing interest

The authors declare that they have no known competing financial interests or personal relationships that could have appeared to influence the work reported in this paper.

Data availability

Data will be made available on request.

Acknowledgements

This research was supported by the Basic Science Research Program of the National Research Foundation of Korea (NRF) funded by the Ministry of Education (2021R1I1A3A04037486), and the NRF funded by the Korean government (MSIT) (2021R1A2C1008368).

Appendix A. Supplementary data

Supplementary data to this article can be found online at https://doi.org/10.1016/j.bioflm.2023.100165.

References

[1] Hubbard TP, Chao MC, Abel S, Blondel CJ, Abel zur Wiesch P, Zhou X, Davis BM, Waldor MK. Genetic analysis of *Vibrio parahaemolyticus* intestinal colonization. Proc Natl Acad Sci USA 2016;113(22):6283–8. https://doi.org/10.1073/pnas.1601718113.

[2] Han N, Mizan MFR, Jahid IK, Ha S-D. Biofilm formation by *Vibrio parahaemolyticus* on food and food contact surfaces increases with rise in temperature. Food Control 2016;70:161–6. https://doi.org/10.1016/j.foodcont.2016.05.054.

[3] World Health Organization. Advances in science and risk assessment tools for *Vibrio parahaemolyticus* and *V. vulnificus* associated with seafood: meeting report. vol. 35. Food & Agriculture Organization; 2021.

[4] Beshiru A, Igbinosa EO. Surveillance of *Vibrio parahaemolyticus* pathogens recovered from ready-to-eat foods. Sci Rep 2023;13(1):4186. https://doi.org/10.1038/s41598-023-31359-4.

[5] Chen X, Li Y, Yao W, Wu T, Zhu Q, Zhang Y, Ye H, Wang R, Zheng S, Yu F. A new emerging serotype of *Vibrio parahaemolyticus* in China is rapidly becoming the main epidemic strain. Clin Microbiol Infection 2020;26(5). https://doi.org/10.1016/j.cmi.2019.09.024. 644-e641.

[6] Ashrafudoulla M, Mizan MFR, Park H, Byun K-H, Lee N, Park SH, Ha S-D. Genetic relationship, virulence factors, drug resistance profile and biofilm formation ability of *Vibrio parahaemolyticus* isolated from mussel. Front Microbiol 2019;10:513. https://doi.org/10.3389/fmicb.2019.00513.

[7] Wang D, Fletcher GC, Gagic D, On SLW, Palmer JS, Flint SH. Comparative genome identification of accessory genes associated with strong biofilm formation in *Vibrio*

parahaemolyticus. Food Res Int 2023;166:112605. https://doi.org/10.1016/j.foodres.2023.112605.
[8] Sharma D, Misba L, Khan AU. Antibiotics versus biofilm: an emerging battleground in microbial communities. Antimicrob Resist Infect Control 2019;8(1):1–10. https://doi.org/10.1186/s13756-019-0533-3.
[9] Mizan MFR, Jahid IK, Ha S-D. Microbial biofilms in seafood: a food-hygiene challenge. Food Microbiol 2015;49:41–55. https://doi.org/10.1016/j.fm.2015.01.009.
[10] Yu H, Rhee MS. Characterization of ready-to-eat fish surface as a potential source of contamination of *Vibrio parahaemolyticus biofilms*. Food Res Int 2023;169:112890. https://doi.org/10.1016/j.foodres.2023.112890.
[11] Wang D, Flint SH, Palmer JS, Gagic D, Fletcher GC, On SLW. Global expansion of *Vibrio parahaemolyticus* threatens the seafood industry: perspective on controlling its biofilm formation. LWT 2022;158:113182. https://doi.org/10.1016/j.lwt.2022.113182.
[12] Wang J, Zhan Y, Sun H, Fu X, Kong Q, Zhu C, et al. Regulation of virulence factors expression during the intestinal colonization of *Vibrio parahaemolyticus*. Foodborne Pathog Dis 2022;19(3):169–78. https://doi.org/10.1016/j.lwt.2022.113182.
[13] Broberg CA, Calder TJ, Orth K. *Vibrio parahaemolyticus* cell biology and pathogenicity determinants. Microb Infect 2011;13(12–13):992–1001. https://doi.org/10.1016/j.micinf.2011.06.013.
[14] Abuga I, Sulaiman SF, Wahab RA, Ooi KL, Rasad MSBA. In vitro antibacterial effect of the leaf extract of *Murraya koenigii* on cell membrane destruction against pathogenic bacteria and phenolic compounds identification. Eur J Integr Med 2020;33:101010. https://doi.org/10.1016/j.eujim.2019.101010.
[15] Mukherjee A, Ghosh S, Ghosh S, Mahato S, Pal M, Sen SK, Majee A, Singh B. Molecular recognition of synthesized halogenated chalcone by calf thymus DNA through multispectroscopic studies and analysis the anti-cancer, anti-bacterial activity of the compounds. J Mol Liq 2021;337:116504. https://doi.org/10.1016/j.molliq.2021.116504.
[16] Raorane CJ, Lee J-H, Kim Y-G, Rajasekharan SK, García-Contreras R, Lee J. Antibiofilm and antivirulence efficacies of flavonoids and curcumin against *Acinetobacter baumannii*. Front Microbiol 2019;10:990. https://doi.org/10.3389/fmicb.2019.00990.
[17] Nag D, Dastidar DG, Chakrabarti G. Natural flavonoid morin showed anti-bacterial activity against *Vibrio cholera* after binding with cell division protein FtsA near ATP binding site. Biochim Biophys Acta - Gen Subj 2021;1865(8):129931. https://doi.org/10.1016/j.bbagen.2021.129931.
[18] Li Q, Yu S, Han J, Wu J, You L, Shi X, Wang S. Synergistic antibacterial activity and mechanism of action of nisin/carvacrol combination against *Staphylococcus aureus* and their application in the infecting pasteurized milk. Food Chem 2022;380:132009. https://doi.org/10.1016/j.foodchem.2021.132009.
[19] Martín-Rodríguez AJ, Ticona JC, Jiménez IA, Flores N, Fernández JJ, Bazzocchi IL. Flavonoids from *Piper delineatum* modulate quorum-sensing-regulated phenotypes in *Vibrio harveyi*. Phytochem 2015;117:98–106. https://doi.org/10.1016/j.phytochem.2015.06.006.
[20] Ruiz-Cruz S, Chaparro-Hernández S, Hernández- Ruiz KL, Cira-Chávez LA, Estrada-Alvarado MI, Gassos Ortega LE, Ornelas-Paz JdJ, Lopez Mata MA. Flavonoids: important biocompounds in food. In: Goncalo CJ, editor. Flavonoids (pp. Ch. 16). Rijeka: IntechOpen; 2017.
[21] Mohd Nasuha NA, Choo Y-M. A new flavone from Malaysia Borneo *Marsdenia tinctoria*. Nat Prod Res 2016;30(13):1532–6. https://doi.org/10.1080/14786419.2015.1118629.
[22] Hossain MK, Choi HY, Hwang J-S, Dayem AA, Kim J-H, Kim YB, Poo H, Cho S-G. Antiviral activity of 3, 4'-dihydroxyflavone on influenza a virus. J Microbiol 2014;52:521–6. https://doi.org/10.1007/s12275-014-4212-z.
[23] Young J-M, Park Y-H, Lee Y-U, Kim H-J, Shim Y-H, Ahn J-H, Lim Y-H. Antimicrobial effects of flavone analogues and their structure-activity relationships. J Microbiol Biotechnol 2007;17(3):530–3.
[24] Kim S, Shin Y, Choi Y, Lim K-M, Jeong Y, Dayem AA, et al. Improved wound healing and skin regeneration ability of 3, 2′-dihydroxyflavone-treated mesenchymal stem cell-derived extracellular vesicles. Int J Mol Sci 2023;24(8):6964. https://doi.org/10.3390/ijms24086964.
[25] Han D, Kim HJ, Choi HY, Kim B, Yang G, Han J, Dayem AA, Lee H-R, Kim JH, Lee K-M. 3, 2/-Dihydroxyflavone-treated pluripotent stem cells show enhanced proliferation, pluripotency marker expression, and neuroprotective properties. Cell Transplant 2015;24(8):1511–32. https://doi.org/10.3727/096368914X683511.
[26] Kim K, Abdal Dayem A, Gil M, Yang G-M, Lee SB, Kwon O-H, Choi S, Kang G-H, Lim KM, Kim D. 3, 2′-Dihydroxyflavone improves the proliferation and survival of human pluripotent stem cells and their differentiation into hematopoietic progenitor cells. J Clin Med 2020;9(3):669. https://doi.org/10.3390/jcm9030669.
[27] Zhu W, Gao J, Liu H, Liu J, Jin T, Qin N, Ren X. Antibiofilm effect of sodium butyrate against *Vibrio parahaemolyticus*. Food Control 2022;131:108422. https://doi.org/10.1016/j.foodcont.2021.108422.
[28] Etayash H, Alford M, Akhoundsadegh N, Drayton M, Straus SK, Hancock REW. Multifunctional antibiotic–host defense peptide conjugate kills bacteria, eradicates biofilms, and modulates the innate immune response. J Med Chem 2021;64(22):16854–63. https://doi.org/10.1021/acs.jmedchem.1c01712.
[29] Antonoplis A, Zang X, Huttner MA, Chong KKL, Lee YB, Co JY, Amieva MR, Kline KA, Wender PA, Cegelski L. A dual-function antibiotic-transporter conjugate exhibits superior activity in sterilizing MRSA biofilms and killing persister cells. J Am Chem Soc 2018;140(47):16140–51. https://doi.org/10.1021/jacs.8b08711.
[30] Liu H, Zhu W, Cao Y, Gao J, Jin T, Qin N, Xia X. Punicalagin inhibits biofilm formation and virulence gene expression of *Vibrio parahaemolyticus*. Food Control 2022;139:109045. https://doi.org/10.1016/j.foodcont.2022.109045.
[31] Mizan MFR, Jahid IK, Kim M, Lee K-H, Kim TJ, Ha S-D. Variability in biofilm formation correlates with hydrophobicity and quorum sensing among *Vibrio parahaemolyticus* isolates from food contact surfaces and the distribution of the genes involved in biofilm formation. Biofouling 2016;32(4):497–509. https://doi.org/10.1080/08927014.2016.1149571.
[32] Yu HH, Song YJ, Yu HS, Lee NK, Paik HD. Investigating the antimicrobial and antibiofilm effects of cinnamaldehyde against *Campylobacter* spp. using cell surface characteristics. J Food Sci 2020;85(1):157–64. https://doi.org/10.1111/1750-3841.14989.
[33] Sathiyamoorthi E, Faleye OS, Lee J-H, Lee J. Hydroquinone derivatives attenuate biofilm formation and virulence factor production in *Vibrio* spp. Int J Food Microbiol 2023;384:109954. https://doi.org/10.1016/j.ijfoodmicro.2022.109954.
[34] Ahmed B, Jailani A, Lee J-H, Lee J. Effect of halogenated indoles on biofilm formation, virulence, and root surface colonization by *Agrobacterium tumefaciens*. Chemosphere 2022;293:133603. https://doi.org/10.1016/j.chemosphere.2022.133603.
[35] Guo M, Fang Z, Sun L, Sun D, Wang Y, Li C, Wang R, Liu Y, Hu H, Liu Y. Regulation of thermostable direct hemolysin and biofilm formation of *Vibrio parahaemolyticus* by quorum-sensing genes *luxM* and *luxS*. Curr Microbiol 2018;75:1190–7. https://doi.org/10.1007/s00284-018-1508-y.
[36] Schwyn B, Neilands JB. Universal chemical assay for the detection and determination of siderophores. Anal Biochem 1987;160(1):47–56. https://doi.org/10.1016/0003-2697(87)90612-9.
[37] Holasová K, Křížkovská B, Hoang L, Dobiasova S, Lipov J, Macek T, Křen V, Valentová K, Ruml T, Viktorova J. Flavonolignans from silymarin modulate antibiotic resistance and virulence in *Staphylococcus aureus*. Biomed Pharmacother 2022;149:112806. https://doi.org/10.1016/j.biopha.2022.112806.
[38] Zhao X, Chen L, Zhao L, He Y, Yang H. Antimicrobial kinetics of nisin and grape seed extract against inoculated *Listeria monocytogenes* on cooked shrimps: survival and residual effects. Food Control 2020;115:107278. https://doi.org/10.1016/j.foodcont.2020.107278.
[39] Li L, Lin Y, Addo KA, Yu Y, Liao C. Effect of allyl isothiocyanate on the growth and virulence of *Clostridium perfringens* and its application on cooked pork. Food Res Int 2023;113110. https://doi.org/10.1016/j.foodres.2023.113110.
[40] Tampakakis E, Okoli I, Mylonakis E. A *C. elegans*-based, whole animal, *in vivo* screen for the identification of antifungal compounds. Nat Protoc 2008;3(12):1925–31. https://doi.org/10.1038/nprot.2008.193.
[41] Kaplan EL, Meier P. Nonparametric estimation from incomplete observations. J Am Stat Assoc 1958;53(282):457–81. https://doi.org/10.1080/01621459.1958.10501452.
[42] Daina A, Michielin O, Zoete V. SwissADME: a free web tool to evaluate pharmacokinetics, drug-likeness and medicinal chemistry friendliness of small molecules. Sci Rep 2017;7(1):42717. https://doi.org/10.1038/srep42717.
[43] Lee M, Lee J, Kim JM, Hong D-H, Chin J, Kim H, Lee J-G, Nam S-J, Yang I, Hahn D. Antibacterial activity of prenylated flavonoids isolated from hop against fish pathogens *Streptococcus iniae* and *Vibrio vulnificus*. Biotechnol Bioproc Eng 2022;27(3):361–9. https://doi.org/10.1007/s12257-021-0247-2.
[44] Lee J-H, Regmi SC, Kim J-A, Cho MH, Yun H, Lee C-S, Lee J. Apple flavonoid phloretin inhibits *Escherichia coli* O157: H7 biofilm formation and ameliorates colon inflammation in rats. Infect Immun 2011;79(12):4819–27. https://doi.org/10.1128/iai.05580-11.
[45] Hammad A, Abutaleb NS, Elsebaei MM, Norvil AB, Alswah M, Ali AO, Abdel-Aleem JA, Alattar A, Bayoumi SA, Gowher H. From phenylthiazoles to phenylpyrazoles: broadening the antibacterial spectrum toward carbapenem-resistant bacteria. J Med Chem 2019;62(17):7998–8010. https://doi.org/10.1021/acs.jmedchem.9b00720.
[46] Kirov SM. Bacteria that express lateral flagella enable dissection of the multifunctional roles of flagella in pathogenesis. FEMS (Fed Eur Microbiol Soc) Microbiol Lett 2003;224(2):151–9. https://doi.org/10.1016/S0378-1097(03)00445-2.
[47] Zha F, Pang R, Huang S, Zhang J, Wang J, Chen M, Xue L, Ye Q, Wu S, Yang M. Proteomic analysis reveals the non-coding small RNA Qrr5 influences autoaggregation and growth competition in *Vibrio parahaemolyticus*. J Proteonomics 2023;279:104866. https://doi.org/10.1016/j.jprot.2023.104866.
[48] Nwoko E-s QA, Okeke IN. Bacteria autoaggregation: how and why bacteria stick together. Biochem Soc Trans 2021;49(3):1147–57. https://doi.org/10.1042/BST20200718.
[49] Defoirdt T. Indole signaling, a promising target to control vibriosis in aquaculture. Amsterdam, Netherlands): Aquaculture; 2023, 739692. https://doi.org/10.1016/j.aquaculture.2023.739692.
[50] Shin HJ, Woo S, Jung GY, Park JM. Indole-3-acetic acid production from alginate by *Vibrio* sp. dhg: physiology and characteristics. Biotechnol Bioproc Eng 2023;28(4):695–703. https://doi.org/10.1007/s12257-023-0056-x.
[51] Salamone M, Nicosia A, Ghersi G, Tagliavia M. *Vibrio* proteases for biomedical applications: modulating the proteolytic secretome of *V. alginolyticus* and *V. parahaemolyticus* for improved enzymes production. Microorganisms 2019;7(10):387. https://doi.org/10.3390/microorganisms7100387.
[52] Shinoda S, Miyoshi S-I. Proteases produced by vibrios. Biocontrol Sci 2011;16(1):1–11. https://doi.org/10.4265/bio.16.1.
[53] Wang R, Sun L, Wang Y, Deng Y, Fang Z, Liu Y, Deng Q, Sun D, Gooneratne R. Influence of food matrix type on extracellular products of *Vibrio parahaemolyticus*. BMC Microbiol 2018;18(1):1–8. https://doi.org/10.1186/s12866-018-1207-7.
[54] Bian N, Chen X, Ren X, Yu Z, Jin M, Chen X, Liu C, Luan Y, Wei L, Chen Y. 7, 8-Dihydroxyflavone attenuates the virulence of *Staphylococcus aureus* by inhibiting alpha-hemolysin. World J Microbiol Biotechnol 2022;38(11):200. https://doi.org/10.1007/s11274-022-03378-2.

[55] Kustusch RJ, Kuehl CJ, Crosa JH. Power plays: iron transport and energy transduction in pathogenic vibrios. Biometals 2011;24:559–66. https://doi.org/10.1007/s10534-011-9437-2.
[56] Meng L, Alter T, Aho T, Huehn S. Gene expression profiles of *Vibrio parahaemolyticus* in viable but non-culturable state. FEMS (Fed Eur Microbiol Soc) Microbiol Ecol 2015;91(5). https://doi.org/10.1093/femsec/fiv035.
[57] Zhang Y, Qiu Y, Xue X, Zhang M, Sun J, Li X, Hu L, Yin Z, Yang W, Lu R. Transcriptional regulation of the virulence genes and the biofilm formation associated operons in *Vibrio parahaemolyticus*. Gut Pathog 2021;13:1–10. https://doi.org/10.1186/s13099-021-00410-y.
[58] Qiao Y, Feng L, Jia R, Luo Y, Yang Q. Motility, biofilm formation and associated gene expression in *Vibrio parahaemolyticus* impaired by co-culture with live *Ulva fasciata*. J Appl Microbiol 2022;132(1):101–12. https://doi.org/10.1111/jam.15175.
[59] Guo Y, Ding S-J, Ding X, Liu Z, Wang J-L, Chen Y, Liu P-P, Li H-X, Zhou G-H, Tang C-B. Effects of selected flavonoids on cell proliferation and differentiation of porcine muscle stem cells for cultured meat production. Food Res Int 2022;160:111459. https://doi.org/10.1016/j.foodres.2022.111459.
[60] Kónya K, Pajtás D, Kiss-Szikszai A, Patonay T. Buchwald–Hartwig reactions of monohaloflavones. Eur J Org Chem 2015;2015(4):828–39. https://doi.org/10.1002/ejoc.201403108.
[61] Moorkoth S, Srinivasan KK, Gopalan Kutty N, Joseph A, Naseer M. Synthesis and evaluation of a series of novel imidazolidinone analogues of 6-aminoflavone as anticancer and anti-inflammatory agents. Med Chem Res 2013;22:5066–75. https://doi.org/10.1007/s00044-013-0486-7.
[62] Muncke J. Endocrine disrupting chemicals and other substances of concern in food contact materials: an updated review of exposure, effect and risk assessment. J Steroid Biochem Mol Biol 2011;127(1–2):118–27. https://doi.org/10.1016/j.jsbmb.2010.10.004.
[63] Burdock GA, Pence DH, Ford RA. Safety evaluation of benzophenone. Food Chem Toxicol 1991;29(11):741–50. https://doi.org/10.1016/0278-6915(91)90182-7.